

Study on the Thermal Conductive Polyoxymethylene/Graphite Composites

Xiaowen Zhao, Lin Ye

The State Key Laboratory of Polymer Materials Engineering, Polymer Research Institute of Sichuan University, Chengdu, 610065

Received 11 April 2008; accepted 23 July 2008

DOI 10.1002/app.29065

Published online 13 October 2008 in Wiley InterScience (www.interscience.wiley.com).

ABSTRACT: The thermal conductive composites of polyoxymethylene (POM)/graphite were prepared through four intercalation methods, including melt (MI), solution (SM), pan milling (SMI), and *in situ* intercalation (IM). For the purpose of improving the interfacial compatibility of POM/graphite, realizing the exfoliation and nano-dispersion of graphite in POM matrix, the effect of the type and the content of the graphite, the nature of the coupling agents used in graphite modification on the properties of the composites was studied. The results showed that the thermal conductive properties of POM were improved remarkably from the value of 0.36 W/(m K) for neat POM to the value of 1.15 W/(m K) in presence of 30 wt %

graphite, and the composites filled with the coupling agent T-1 or T-2 surface-modified colloidal graphite displayed better thermal conductivity. The degree of layers exfoliation of the graphite was enhanced in the order of MI, SM, SMI, and IM. And the composites prepared by SM, SMI, and IM methods presented much more decreased size, more narrow size distribution, thinner overlapped sheets, and better dispersion of the graphite than that prepared by MI method. © 2008 Wiley Periodicals, Inc. *J Appl Polym Sci* 111: 759–767, 2009

Key words: polyoxymethylene (POM); graphite; nano-composites; thermal conductivity

INTRODUCTION

Polyoxymethylene (POM), as an engineering plastic with excellent performance, has a wide range of applications in industry, for example, in electrical and electronic applications, automotive applications, and precision machine applications.^{1,2} It not only has high mechanical strength, excellent abrasion resistance, fatigue resistance, and moldability, but also possesses relatively high thermal conductivity. Although much effort has been devoted to improve the mechanical properties and thermal stability of POM, little information is available for the POM based thermal conductive composites.

Graphite is a naturally abundant material and has been considered as an ideal candidate for manufacturing thermal conductive polymer composites because of its light-weight, high thermal conductivity (110–130 W/(m K) at room temperature) and a unique layered nano-structure. It is suggested that in

the case of ductile materials, fillers with platelet shape offer advantages over other spherical or cylindrical morphologies because they can overlap with a large contact area permitting much closer contact between adjacent platelets and reducing the thermal contact resistance. For graphite, the carbon atoms are bonded covalently in a hexagonal arrangement within its crystal layers and these layers are bonded to each other by weak van der Waals forces. The *d*-spacing between the carbon layers is 0.335 nm, and it is possible for a wide range of atoms, ions, and molecules to intercalate between graphite layers and form the graphite intercalation compounds.^{3–5} In the past two decades, various polymer/graphite thermal conductive composites have been developed. Early in 1991, Agari et al. reported the thermal conductive behavior of PE/graphite composite with a thermal conductivity of 1.53 W/(m K) when 20 vol % graphite was added.⁶ After that, Krupa and Chodak investigated the thermal conductivity of polystyrene/graphite composites and a thermal conductivity of 0.7 W/(m K) was obtained when 20 vol % graphite was added.⁷ However, within these researches little investigation deals with POM/graphite thermal conductive composites.

In this work, graphite was compounded with POM to prepare the thermal conductive composites. The thermal conductive properties of POM were tried to be improved without much more sacrificing its mechanical properties and the application area of

Correspondence to: L. Ye (yelinwh@126.com).

Contract grant sponsor: Program for Changjiang Scholars and Innovative Research Team in University; contract grant number: IRT0449.

Contract grant sponsor: New-Century Training Program Foundation for the Talents; contract grant number: NCET-07-0589.

POM would be expected to be enlarged. For example, in electronic industry, the new applications of dissipating the heat and maintain the operating temperature require new composites with high thermal conductivity.

EXPERIMENTAL

Materials

The POM used in this study is a commercial grade powder without any additives and supplied by Yuntianhua Co. Ltd (Yunnan, China). It is a copolymer with a melt flow index of 9.0 g/10 min (M90). A series of titanate coupling agents was kindly provided by Changzhou Jinai Additives Co. Ltd. Colloidal graphite and nano-graphite with the average diameter of 4 μm and 200 nm, respectively, as well as other chemical agents are all commercial grade products and used without further purification.

Surface modification of the graphite

The surface modification of the graphite was carried out by using varying titanate coupling agents. First, ethyl alcohol solution of the coupling agent was prepared, and then a certain amount of graphite was added to the solution. After ultrasonic irradiation at 50°C for 0.5–1 h, the resulting suspension was filtered, then dried in the vacuum oven at 80°C for 5 h, and finally the modified graphite was obtained.

Preparation of the POM/graphite composites

POM/graphite composites were prepared by the following four methods:

1. Melt processing intercalation (MI): the specimens were prepared by dispersing graphite in melted POM.
2. *In situ* intercalative polymerization/melt processing (IM): The monomers of 1, 3, 5-trioxane and 1, 3-dioxolane were mixed with graphite, catalyzed with $(\text{C}_2\text{H}_5)_2\text{O BF}_3$, and *in situ* polymerized at 65°C. Afterwards, it was compounded and melt processed with POM.
3. Solvent intercalation/melt processing (SM): graphite was dispersed in phenylcarbinol by introduction of ultrasonic irradiation, and then the POM powder was dissolved in the dispersion system. The POM/graphite composite was precipitated, washed and dried. Then, it was compounded and melt processed with POM.
4. Solid-state pan milling intercalation/melt processing (SMI): The mixture of POM powder and graphite was milled by three dimensional

grinding discs for appropriate time, and then it was compounded and melt processed with POM.

Measurements

Thermal conductive property

The thermal conductive properties of the composites were measured with a Hot Disk thermal analyser (Hot Disk AB, Uppsala/Sweden), which was based upon a transient technique.⁸

Mechanical property

The tensile strength of the samples was measured with a 4302 material testing machine from Instron Co. (USA.) according to ISO527/1-1993 (E). The notched charpy impact strength of the samples was measured with ZBC-4B impact testing machine from Xinsansi Co. (Shenzhen of China) according to ISO179-1993 (E).

Wide angle X-ray diffraction analysis (Waxd)

WAXD scans were performed with RigakuD/max-III B diffractometer (Japan) through reflection mode. The *d*-spacing of graphite layers can be calculated with the Bragg equation:

$$2d \sin \theta = n\lambda \quad (1)$$

where θ is the Bragg angle, n is the order of diffraction, and λ is the incident wave length.

Scanning electron microscopy analysis

The surface morphology analysis of the tensile fractured samples was performed with JEOL JSM-5900LV scanning electron microscopy (SEM) (Japan). The operating voltage was 20 KV.

RESULTS AND DISCUSSION

Effect of the type of the coupling agents on the properties of POM/nano-graphite composites

It is difficult to disperse the graphite uniformly in polymer matrix because of their incompatibility; thus, the improvement of the compatibility between graphite and polymer is important. Treatment with coupling agent is one of the most commonly used methods for surface modification of graphite and promoting favorable interactions between the polymer matrix and the graphite. In this work, nano-graphite was modified with varying titanate coupling agents to enhance the compatibility between the graphite and the POM matrix, as well as

TABLE I
The Type of Titanate Coupling Agents

Titanate coupling agent	Type of titanate coupling agent	Molecular structure character
T-1	Alcohol amino titanate	Alcohol + amino group
T-2	Alcohol amino titanate	Alcohol + amino group
T-3	Alkyl-sulfonyl titanate	Sulfonyl group
T-4	Pyrophosphate titanate	Pyrophosphate group
T-5	Pyrophosphate titanate	Pyrophosphate + acetate group

preventing from the agglomerations of the graphite. Ultrasonic irradiation was applied in this modification process to promote the dispersion and exfoliation of the nano-graphite.^{9,10}

The type of the coupling agents used in this work was listed in Table I, in which T-1 and T-2 contained alcohol amino basic group, T-3 contained sulfonyl group, T-4 contained pyrophosphate group, and T-5 contained pyrophosphate and acetate group. The effect of the coupling agents on the thermal conductive properties as well as the mechanical properties of POM/nano-graphite composites was investigated. It was found that during the extrusion processing of the composites, POM/nano-graphite modified with T-3, T-4, and T-5 degraded seriously and even could not be hauled and granulated, which may be attributed to the acid products from the hydrolysis of acid esters group in the molecules of these coupling agents, whereas no degradation occurred for the extrusion processing of the composites with the graphite modified by T-1 and T-2 because they contained alcohol amino basic group instead of acid esters group.

The effect of the coupling agents on the thermal conductive properties of POM/nano-graphite composites was shown in Table II. The results showed that the thermal conductivity of POM was improved remarkably in presence of graphite and about 70% increase of the thermal conductivity can be achieved for the composite with 10 wt % graphite. However, the thermal conductivity of the composites was close to each other for the graphite modified with varying coupling agents, indicating that the coupling agents

TABLE II
Effect of Coupling Agents on the Thermal Conductive Properties of POM/nano-Graphite Composites

Samples	Thermal conductivity (W/(m K))	Thermal diffusivity (m ² /s)
POM	0.33	0.19
POM/10 wt % nano-graphite	0.55	0.42
POM/10 wt % nano-graphite/T-1	0.56	0.51
POM/10 wt % nano-graphite/T-2	0.55	0.46

TABLE III
Effect of Coupling Agents on the Mechanical Properties of POM/nano-Graphite Composites

Samples	Tensile strength (MPa)	Elongation at break (%)	Notched charpy impact strength (KJ/m ²)
POM	60.16	40.0	7.01
POM/10 wt % nano-graphite	63.61	3.8	6.56
POM/10 wt % nano-graphite/T-1	62.55	14.4	6.20
POM/10 wt % nano-graphite/T-2	61.81	17.1	6.70

had no or negligible influence on the thermal conductivity of the composites. The thermal diffusivity related to the microscopic transport of heat was also a representation of the thermal conductive properties of materials. As shown in Table II, the thermal diffusivity of POM was also improved remarkably in presence of graphite.

The effect of the coupling agents on the mechanical properties of POM/nano-graphite composites was shown in Table III. In comparison with neat POM, there was a little change of the tensile strength and a large drop in elongation at break for POM/nano-graphite composites. The charpy notched impact strength of POM also decreased to a certain degree in presence of graphite. However, this impair in the toughness of the composites can be reduced dramatically by using graphite modified with T-1 and T-2, suggesting that the surface modification of the graphite with these two coupling agents was efficient.

The alcohol amino titanate coupling agents, T-1 and T-2, were enriched with amino groups, which had great affinity with POM. As shown in Figure 1, it was easy for such coupling agent to form the hydrogen bond with the molecules of POM. Therefore, the interfacial adhesion and compatibility

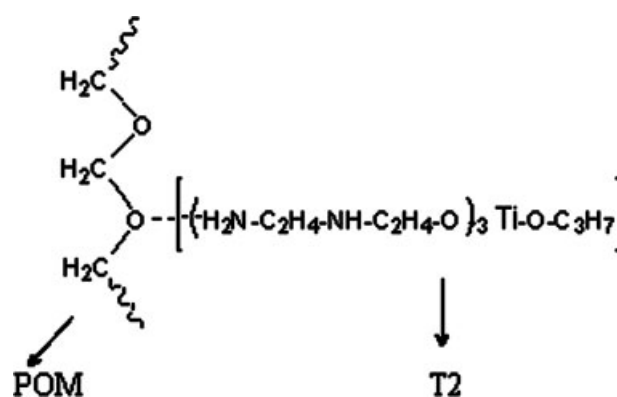


Figure 1 Hydrogen bonding interaction of POM with the coupling agents.

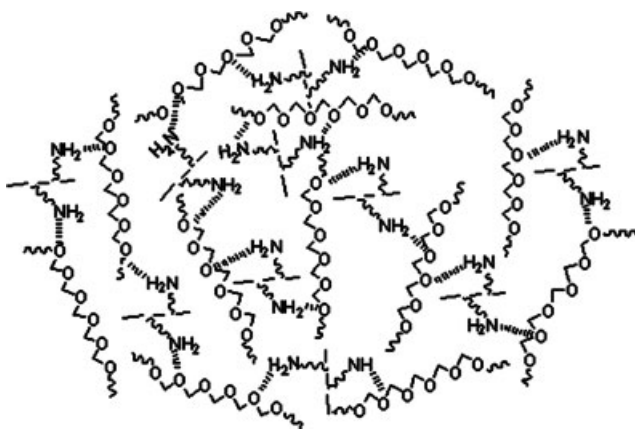


Figure 2 The schematic illustration of the network formed between the macromolecules of POM and the modified graphite sheets.

between graphite and POM were improved, the interfacial stress tended to be more transmissible and homogenized, and finally the mechanical properties of POM were enhanced. Figure 2 represented the graphite layers bridged network formed through hydrogen bonding between the POM molecules and the modified graphite sheets.

Effect of the type of the graphite on the properties of POM/graphite composites

There were a lot of varieties of graphite, in which natural flake graphite was widely used as the conductive fillers for its very high thermal conductivity. Nano-graphite and colloidal graphite used in this work were both fabricated by purifying natural flake graphite and possessed small particle size and high thermal conductivity. As shown in Figure 3, the thermal conductivity and thermal diffusivity of the composites filled with colloidal graphite were higher than that of the composites filled with nano-graphite for the same graphite content, indicating that the contribution of these two types of graphite to the thermal conductive properties of the composites was

different. The colloidal graphite had more perfect crystal structure, which was beneficial to phonon transport in graphite and more conductive paths can be created. The larger particle size of the colloidal graphite flakes had larger aspect ratios, which provided a better structure to form a conducting network.

As shown in Figure 4, it can be seen that the tensile strength, elongation at break, and impact strength of the composite filled with the nano-graphite were higher than that of the composite filled with the colloidal graphite, perhaps because of the relatively small particle size of the nano-graphite.

Effect of the content of graphite on the properties of POM/graphite composites

The thermal conductive properties of POM/graphite composites versus graphite content were shown in Figure 5. For both investigated systems, a nonlinear increase of the thermal conductivity and diffusivity was observed with an increase of the content of graphite. The thermal conductivity increased from the value of 0.36 W/(m K) for neat POM to the value of 1.15 W/(m K) in presence of 30 wt % colloidal graphite, and 1.05 W/(m K) in presence of nano-graphite. It also can be seen that the composites filled with colloidal graphite displayed better thermal conductive properties than that filled with nano-graphite for varying graphite content. This difference was more significant for the composites at higher filler content. Maxwell-Eucken model¹¹ was used to evaluate the thermal conductivity of the composites.

$$\lambda = \frac{\lambda_p [2\lambda_p + \lambda_f + 2V_f(\lambda_f - \lambda_p)]}{2\lambda_p + \lambda_f - V_f(\lambda_f - \lambda_p)} \quad (2)$$

where λ , λ_p , and λ_f are the thermal conductivity of composites, polymer, and filler, respectively; and V_f is the volume fraction of filler.

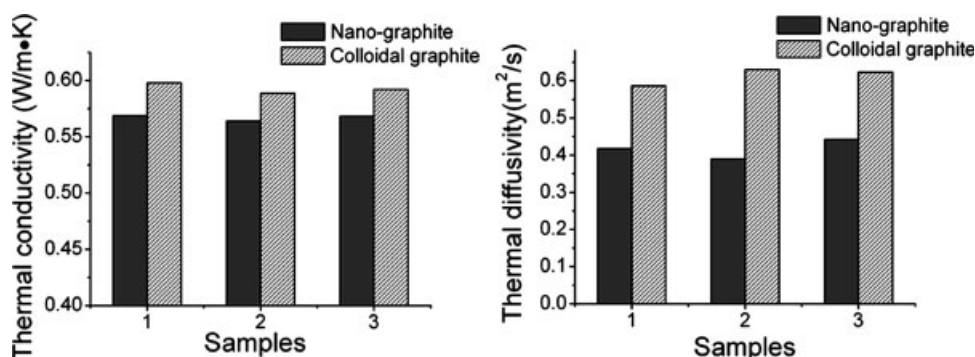


Figure 3 Effect of graphite type on the thermal conductive properties of POM/10 wt % graphite composites (1: POM/graphite; 2: POM/graphite/T-1; 3: POM/graphite/T-2).

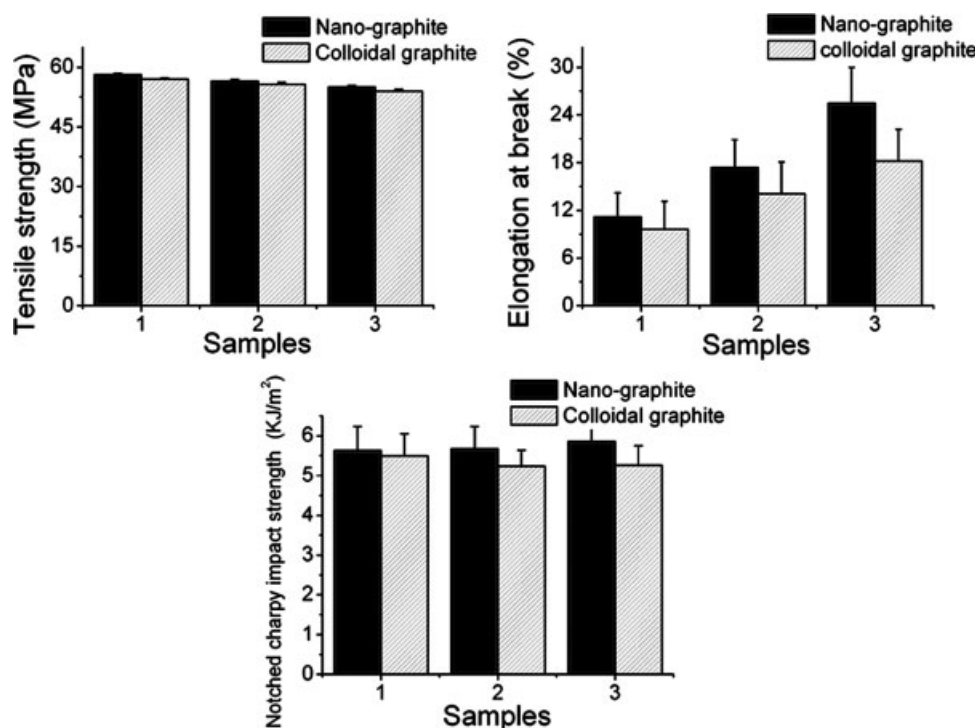


Figure 4 Effect of graphite type on the mechanical properties of POM/10 wt % graphite composites (1: POM/graphite; 2: POM/graphite/T-1; 3: POM/graphite/T-2).

As shown in Figure 6, it was clear that the experimental data did not agree with Maxwell-Eucken model very well, and the experimental data were

always higher than those predicted. The model assumed that the filler was spherical, and confined to common dispersion state in the polymer matrix. However, the graphite possessed layer structures and the much better dispersion state of the filler formed through ultrasonic irradiation was obviously beyond the presuming limit of the model, resulting in the improvement of the thermal conductivity of the composites even at low filler content.

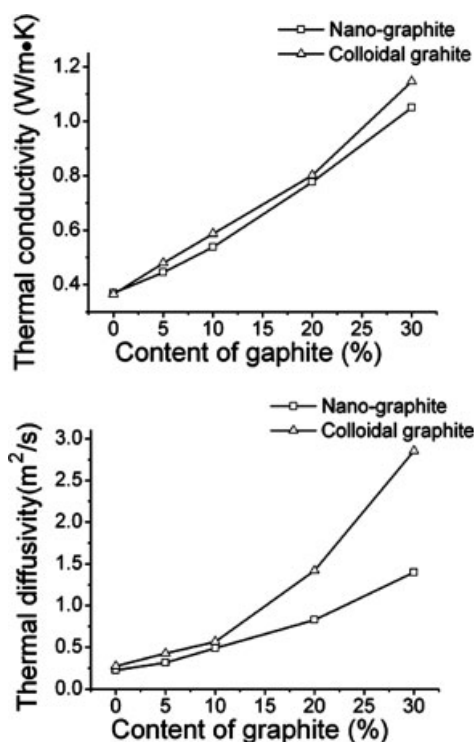


Figure 5 Effect of the content of graphite on the thermal conductive properties of POM/graphite/T-2 composites.

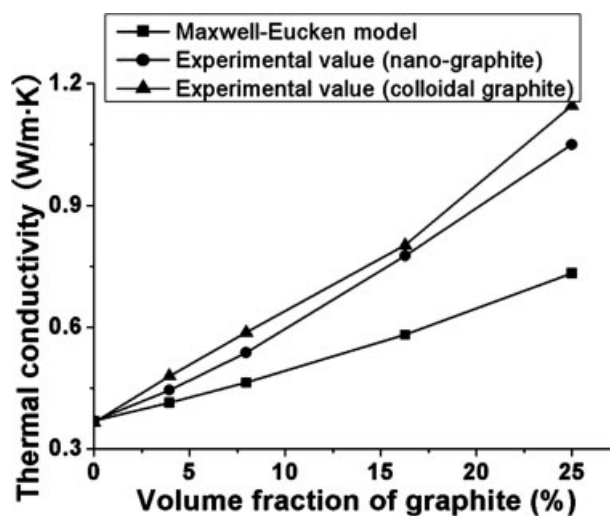


Figure 6 Comparison of experimental and predicted thermal conductivity of POM/graphite/T-2 composites.

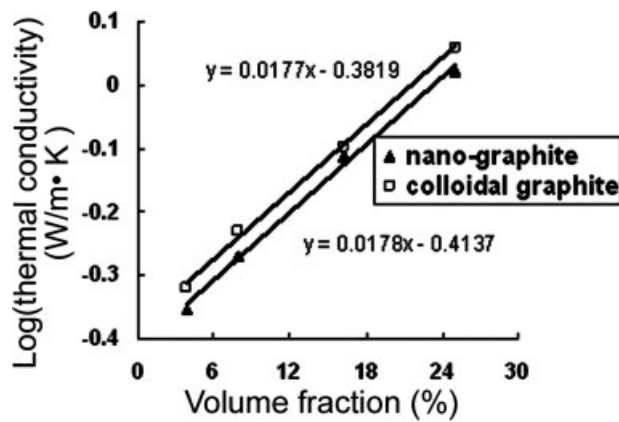


Figure 7 Logarithms for thermal conductivity of POM/graphite/T-2 composites: experimental data and Agari's model.

The model of Agari¹²⁻¹³ was applied to investigate the effect of the type of the graphite on the thermal conductivity of composites, which considered the effect of the dispersion state by introducing two factors C_1 and C_2 :

$$\log \lambda = V_f C_2 \log \lambda_f + (1 - V_f) \log (\lambda_p C_1) \quad (3)$$

where λ , λ_p , and λ_f are the thermal conductivity of composites, polymer, and filler, respectively; V_f , the volume fraction of filler; C_1 , a factor relating to the structure of polymer, such as crystallinity of matrix; and C_2 , a factor relating to the measure of ease for the formation of conductive chains of filler. Accord-

TABLE IV
 C_1 and C_2 of Agari Model for POM/Graphite Composites

Composites	C_1	C_2
POM/colloidal graphite	1.12	0.666
POM/nano-graphite	1.04	0.655

ing to Agari model, the closer C_2 values is to 1, the more easily conductive chains are formed in composites. Therefore, the thermal conductivity of composites may vary with the dispersion state of fillers, even if for the same composition of the composites. As shown in Figure 7 and Table IV, by fitting the experimental data for the model, the value of C_1 and C_2 for the above two systems, and a possible explanation of the dispersion state of filler in composites could be obtained.

It was observed that the type of graphites can affect the values of C_1 and C_2 , which suggested that the crystalline structure of the composite was influenced by the type of the graphite and a better dispersion state of the graphite was achieved in the POM/colloidal graphite composites. Therefore it was more likely for the formation of conductive channels in the POM/colloidal graphite composites.

The dependence of mechanical properties of the composites on the graphite content was shown in Figure 8. There was a small change for their tensile strength with an increase of graphite content. A steep decrease of elongation at break and notched impact strength was observed for both investigated

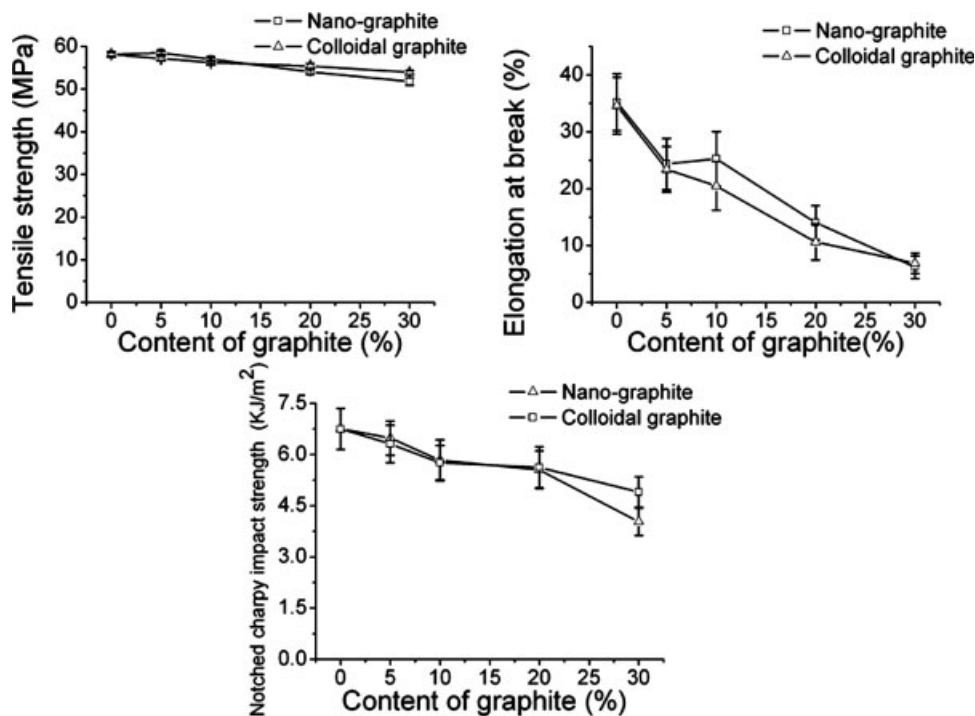


Figure 8 Effect of the content of the graphite on the mechanical properties of POM/graphite/T-2 composites.

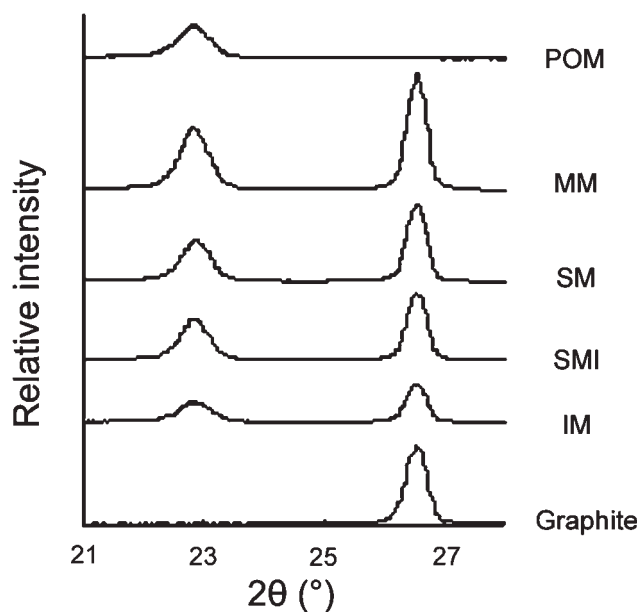


Figure 9 Wide angle X-ray diffraction pattern of graphite and POM/10 wt % colloidal graphite/T-2 prepared by different methods.

systems. The presence of a filler in the matrix resulted, besides a reinforcing effect, also in a formation of sites of stress concentration. Especially at high filler content, large numbers of sites of stress concentration were formed, which were in close vicinity and the crack, once formed, can propagate rapidly through the sample. Therefore, in this case the specimens may break at low deformation. Nevertheless, the composite with 30 wt % graphite maintained relatively high tensile strength and impact toughness.

Effect of the preparation methods on the morphology and properties of POM/graphite composites

The morphology and properties of POM/graphite were substantially affected by the dispersion of graphite in POM matrix. In this section, four different methods, the melt intercalation (MI), *in situ* intercalative polymerization/melt processing (IM), solvent intercalation/melt processing (SM), and

solid-state pan milling/melt processing (SMI) were applied to the preparation of POM/colloidal graphite composites to achieve the good dispersion and exfoliation of graphite in POM matrix.

Wide angle X-ray diffraction (WAXD) analysis

Wide angle X-ray diffraction (WAXD) analysis was performed to evaluate the structure, the degree of expansion, and exfoliation of graphite particles in the composites. Figure 9 showed the WAXD patterns of POM/graphite (10 wt %) composites prepared by MI, SM, SMI, and IM intercalation methods. The WAXD patterns for neat POM and pure graphite were also plotted for comparison. While neat POM showed a broad peak at 23°, the composites presented a new sharp peak at 2θ of about 26.5° besides the diffraction peak attributed to the neat POM. This new diffraction peak corresponded to a *d*-spacing of 3.35 Å, which was also the characteristic peak of pure graphite. The occurrence of this peak confirmed not only the presence of graphite in the composites, but also the fact that the individual graphite nano-sheets consisted of multilayer of graphite. Therefore, it can be suggested that the intercalation methods applied here could not exfoliate or separate the graphite layers completely. Moreover, the high intensity of the diffraction peak indicated the large number of multilayer of graphite in the composites. As shown in Figure 9 and Table V, the diffraction peak intensity of graphite in the composites decreased in the order of MI, SM, SMI and IM methods, indicating that the degree of layers exfoliation of the graphite increased in turn.

The crystallinity of Waxd method was given as the follow expression:

$$\text{Crystallinity (\%)} = S_c / (S_c + S_a) \times 100 (\%)$$

where S_c is the area under the crystalline curve and S_a is the area under the amorphous curve.

As shown in Table V, compared with the neat POM, the crystallinity of POM decreased in presence of the graphite suggesting that graphite can hinder the movement of macromolecular chains, make the

TABLE V
2θ and Interlayer Distance of the Graphite Layers

Preparation method	(002) peak position 2θ (°)	(002) plane spacing <i>d</i> (Å)	(002) peak height H_p (counts/s)	Crystallinity of the composites (%)
Graphite	26.5362	3.3562	135308.20	65
POM/graphite/T-2 (MI)	26.5288	3.3572	40037.31	50
POM/graphite/T-2 (SM)	26.5106	3.3595	28126.25	54
POM/graphite/T-2 (SMI)	26.5159	3.3588	24062.36	52
POM/graphite/T-2 (IM)	26.5076	3.3599	13807.90	54

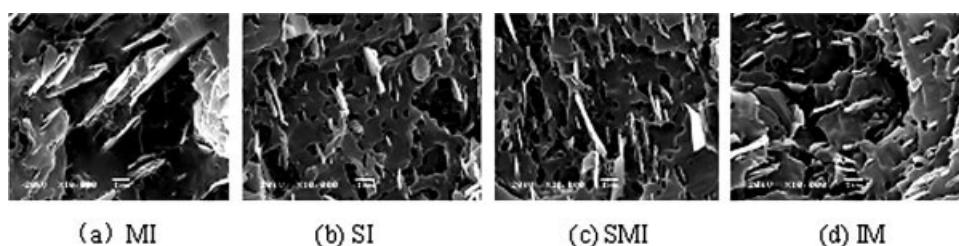


Figure 10 SEM micrographs of POM/10 wt % colloidal graphite/T-2 composites.

chain folding process quite difficult, and therefore decrease the crystallization performance of POM.

The morphology of POM/colloidal graphite composites

The morphology of POM/graphite composites prepared by different methods at 10 wt % of graphite was studied by SEM. Agglomerates of graphite and large flat graphite platelets were present obviously in the samples prepared by MI method, as shown in Figure 10(a), whereas the graphite agglomerates was broken down for the samples prepared by SM, SMI, and IM methods, resulting in a better dispersed system free of particle agglomerations with the graphite platelets being well embedded in POM matrix, as shown in Figure 10(b–d). It was concluded that except for MI method, all other intercalation methods can provide enough shear stress to break down the graphite agglomerates and promote the graphite platelets to disperse homogeneously.

Thermal conductive properties and mechanical properties

The thermal conductive properties of the composites prepared by MI, SM, SMI, and IM methods were quite different as shown in Table VI, indicating that the preparation method had a great effect on the dispersion of the graphite in POM matrix. It should be noted that the one prepared by SM method had better thermal conductive properties.

Table VII displayed the mechanical properties of POM/graphite composites prepared by different

methods with a graphite content of 10 wt %. It should be noted that the one prepared by SMI had better mechanical properties.

CONCLUSIONS

Graphite was applied to be compounded with POM to prepare thermal conductive nano-composites. In presence of graphite, the thermal conductive properties of POM were improved remarkably. The composites filled with the coupling agents T-1 or T-2 surface-modified colloidal graphite displayed relatively high thermal conductivity, which increased from the value of 0.36 W/(m K) for neat POM to the value of 1.15 W/(m K) in presence of 30 wt % colloidal graphite, and the composite maintained relatively high mechanical properties. Both the Maxwell-Eucken model and Agari model were used to evaluate the thermal conductivity of the composites. The experimental data were always higher than those predicted owing to the layer structures and the much better dispersion state of the graphite formed through ultrasonic irradiation. Examining the parameters of the Agari model indicated that the crystalline structure of the composite was influenced by the type of the graphite and a better dispersion state of the graphite was achieved in the POM/colloidal graphite composites. The XRD analysis showed that the diffraction peak intensity of (002) crystal plane of the graphite in the composites decreased in the order of MI (melt), SM (solution), SMI (pan milling), and IM (*in situ* intercalation), which indicated that

TABLE VI
Effect of the Intercalation Methods on the Thermal Conductive Properties of POM/Colloidal Graphite Composites

Samples	Thermal conductivity (W/(m K))	Thermal diffusivity (m ² /s)
POM	0.37	0.23
MI-POM/10 wt % graphite/T-2	0.59	0.62
SM-POM/10 wt % graphite/T-2	0.68	0.69
SMI-POM/10 wt % graphite/T-2	0.55	0.56
IM-POM/10 wt % graphite/T-2	0.60	0.75

TABLE VII
Effect of the Intercalation Methods on the Mechanical Properties of POM/Colloidal Graphite Composites

Samples	Tensile strength (MPa)	Elongation at break (%)	Notched charpy impact strength (KJ/m ²)
MI-POM/10 wt % graphite/T-2	58.98	18.18	5.26
SM-POM/10 wt % graphite/T-2	58.63	12.66	5.46
SMI-POM/10 wt % graphite/T-2	58.91	20.61	5.94
IM-POM/10 wt % graphite/T-2	61.27	12.21	3.94

the degree of layers exfoliation of the graphite was enhanced in turn. The SEM analysis showed that compared with MI method, the composites prepared by SM, SMI, and IM methods presented much more decreased size, more narrow size distribution, thinner overlapped sheets, and better dispersion of the graphite. The composites prepared by SM method had relatively high thermal conductive properties and the composites prepared by SMI method had relatively high mechanical properties.

References

1. Hasegawa, S.; Takeshita, H.; Yoshii, F.; Nishimoto, S. *Polymer* 2000, 41, 111.
2. Hisakatsu, H.; Kohji, T. *Polymer* 2003, 44, 3107.
3. Kalaitzidou, K. PhD Thesis, Michigan State University, East Lansing, MI, 2006.
4. Nielsen, L. E. *J Appl Polym Sci* 1973, 17, 3819.
5. Hill RF. PhD Thesis, Institut für Struktur- und Funktionskeramik Montanuniversität, Leoben, Austria, 2002.
6. Agari, Y.; Ueda, A.; Nagai, S. *J Appl Polym Sci* 1991, 42, 665.
7. Krupa, I. C. *Euro Polym J* 2001, 37, 2159.
8. Qi, W.; Hesheng, X.; C. Z. *J Appl Polym Sci* 2001, 80, 1478.
9. Suslick, K. S.; Cline Jr., R. E.; Hammerton, D. A. *J Am Chem Soc* 1986, 108, 5641.
10. Suslick, K. S.; Didenko, Y.; Fang, M. M.; Hyeon, T.; Kolbeck, K. J.; McNamara III, W. B.; Mdeleleni, M. M.; Wong, M. *Philos Trans R Soc of London, Series A* 1999, 357, 335.
11. Sim, L. C.; Ramanan, S. L.; Ismail, H. *Thermochim Acta* 2005, 430, 155.
12. Agari, Y.; Ueda, A.; Nagai, S. *J Appl Polym Sci* 1993, 49, 1625.
13. Agari, Y.; Ueda, A.; Nagai, H. *J Appl Polym Sci* 1991, 43, 1117.